

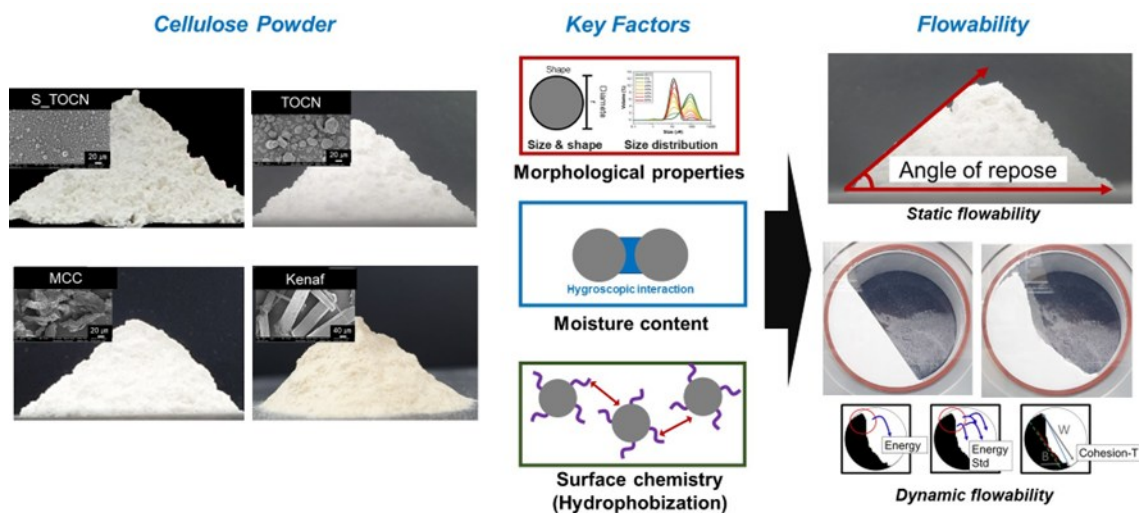
Flowability of Cellulose Powder Depending on the Morphology and Hydrophobicity

Hakmyoung Lee ,^a Heenae Shin,^b Shin Young Park,^c Yujin Oh,^a Jinseung Kim,^a and Hye Jung Youn ,^{a,b,*}

* Corresponding author: page94@snu.ac.kr

DOI: 10.15376/biores.21.1.1397-1412

GRAPHICAL ABSTRACT



Flowability of Cellulose Powder Depending on the Morphology and Hydrophobicity

Hakmyoung Lee ,^a Heenae Shin,^b Shin Young Park,^c Yujin Oh,^a Jinseung Kim,^a and Hye Jung Youn ,^{a,b,*}

Flowability is an essential property that must be evaluated to ensure smooth and consistent feeding of powder materials into hoppers. However, the flowability of cellulose powders is difficult to predict due to their complex particle morphology and surface characteristics. In this study, the key factors affecting the flowability of cellulose powders, including particle size, shape, size distribution, moisture content, and surface chemistry, were investigated using cellulose nanofiber, microcrystalline cellulose, and kenaf pulp. Both static and dynamic flowability were evaluated using angle of repose measurements and dynamic avalanche analysis. Among the morphological factors, the average particle size of cellulose powders was identified as the dominant parameter influencing their flowability. Flowability improved with increasing particle size and showed a sharp decline for fine particles smaller than 70 μm . With increasing moisture content, the flowability of fine particles smaller than 20 μm was improved, whereas that of relatively larger particles deteriorated. Hydrophobization enhanced flowability by reducing surface energy and friction. However, excessive hydrophobization induced particle aggregation and decreased flowability. These results identified the key parameters governing cellulose powder flow and clarify the characteristics advantageous for stable feeding and uniform product quality.

DOI: 10.15376/biores.21.1.1397-1412

Keywords: Cellulose; Powder; Flowability; Avalanche behavior; Angle of repose

Contact information: a: Department of Agriculture, Forestry and Bioresources, Seoul National University, 1 Gwanak-ro, Gwanak-gu, Seoul 08826 Korea; b: Research Institute of Agriculture and Life Sciences, Seoul National University, 1 Gwanak-ro, Gwanak-gu, Seoul 08826 Korea; c: Department of Forest Sciences, Seoul National University, 1 Gwanak-ro, Gwanak-gu, Seoul 08826 Korea;

* Corresponding author: page94@snu.ac.kr

INTRODUCTION

In many industries, most solid materials are used in powder form to facilitate transport, storage, and mixing. To use a powder material effectively, it is necessary to understand the flow characteristics of the powder. When powder flows into hoppers, issues, such as rathole or arching, may occur due to improper flow behavior, and these problems can hinder the production of uniform, high-quality products (Prescott and Barnum 2000). The flow behavior of powder is also a critical issue in a wide range of nano- and meso-particle systems, where powder handling behavior strongly influences processing stability and final material performance (Sharifi *et al.* 2023). Flowability, which can be generally defined as the ability of a powder to flow, refers to the relative movement of particles with respect to surrounding particles or the container. Unlike liquids, predicting the flow

behavior of particulate solids is difficult because powder flowability is influenced by various forces, including gravity, friction, cohesion, and adhesion (Peleg 1977).

There are various methods to evaluate flowability (Shat *et al.* 2023; Brubaker *et al.* 2024). Measuring the angle of repose is a simple and commonly used method (Mehta and Barker 1994; Geldart *et al.* 2006). It refers to the angle formed between the ground and a pile of powder that has fallen from a certain height. This measurement is related to static flowability; however, it is difficult to determine the angle of repose for cohesive or fibrous powder (Horio *et al.* 2014). The shear cell test method involves shearing powder until it flows and measuring friction force (Jenike 1964). An avalanche behavior test is performed in a rotating drum (Hancock *et al.* 2004). The avalanche behavior of powder occurs when the balance between cohesion and gravity force is disrupted (Lavoie *et al.* 2002). Parameters, such as avalanche energy and break energy, can be obtained from avalanche behavior. These parameters are related to the flowability and cohesion of the powder (Trpělková *et al.* 2020). Because this method measures the flow of powder in motion, it can evaluate flowability under conditions similar to real-life situations. Zainuddin *et al.* (2012) developed a vibration shear tube method, which measures the static and dynamic friction of powders using a vibrating tube.

After methods for measuring the flowability were developed, factors affecting flowability have been studied. Stavrou *et al.* (2020) evaluated the effect of particle size on flowability using spherical glass beads by the shear cell test method. They reported that the flowability increases as particle size increases. Horio *et al.* (2014) and Hassan and Lau (2009) investigated the effect of shape and found that spherical powders exhibit good flowability. The size distribution is one of the crucial factors affecting flowability (Liu *et al.* 2008; Kudo *et al.* 2020; Stavrou *et al.* 2020). Powders with small particle size distribution generally have good flowability. Liu *et al.* (2008) reported that ibuprofen powder flowability is greatly influenced by both the particle size and size distribution. The effect of moisture content on the flowability of various cellulose powders was studied in detail by Crouter and Briens (2014). Moisture can reduce or increase the flowability of powders. The moisture can increase cohesion by forming strong liquid bridges (Amidon and Houghton 1995; Crouter and Briens 2014) or reduce electrostatic forces between powders by dissipating charges and acting as a lubricant (Faqih *et al.* 2007). Kim *et al.* (2019) showed that hydrophobization of ceramic tile granule powders can improve the flowability of powders. Li *et al.* (2004) investigated the effect of powder properties for pharmaceutical materials on both flowability and compatibility, which are the two important properties in the tableting process.

Cellulose is a natural polymer with high mechanical strength, chemical stability, biodegradability, and biocompatibility. Because of these properties, cellulose has been applied in biocomposites or pharmaceutical industries (Orts *et al.* 2005; Shokri and Adibkia 2013). Cellulose needs to be prepared in powder form for compounding and industrialization. Varieties of cellulose derivates or nanofibrillated celluloses have been used to tune and improve the properties of composites (Turbak *et al.* 1983; Nevell and Zeronian 1985). Various powdering methods such as milling (Zhang *et al.* 2012) or spray drying (Peng *et al.* 2012) have been developed and used. Due to various influencing factors, the properties of cellulose powder are very complicated, making it difficult to quantitatively evaluate and characterize the flowability. In addition, the hygroscopic nature of cellulose (Zafeiropoulos 2011) may also affect its flowability. As the use of cellulose powder in biocomposites continues to increase, the evaluation of its flowability has become crucial for ensuring process efficiency product quality.

Despite its complicated characteristics, various approaches have been proposed to evaluate the flowability of cellulose powder. To date, static flowability evaluation methods, such as the angle of repose and indices derived from bulk and tapped densities, including Carr's index and the Hausner index, have been most commonly employed (Tasnim *et al.* 2023; Ohwoavworhua *et al.* 2020). In addition, some studies have assessed flowability using custom-built experimental apparatuses. However, because these approaches rely on individually fabricated equipment and specific measurement conditions, it is difficult to obtain standardized and generally comparable flowability values (Genina *et al.* 2009, 2010). Furthermore, such methods mainly focus on macroscopic behaviors, such as the falling rate of fibers, which makes it difficult to analyze flowability from multiple perspectives, including inter-fiber interactions. In addition, most studies investigating the factors influencing the flowability of cellulose powders have examined the effects of individual parameters, such as particle shape and size (Horio *et al.* 2014), moisture content (Sun 2016), and surface modification (Chattoraj *et al.* 2011). Nevertheless, studies that simultaneously compare and analyze these factors under identical experimental conditions are rarely reported (Monroe *et al.* 2025). Because the flowability of cellulose powders can vary significantly depending on both material characteristics and environmental conditions, a comprehensive evaluation under controlled conditions is required.

In this paper, the flowability of cellulose powder produced by various methods was evaluated using both the angle of repose and avalanche behavior to evaluate static and dynamic flow characteristics. Because powder morphology is known to be one of the dominant factors related to flowability (Horio *et al.* 2014), the effects of particle size, aspect ratio, and size distribution were investigated for different types of cellulose, including nanofibrillated cellulose and microcrystalline cellulose. In addition, considering the hydrophilic nature of cellulose, the effect of moisture content was evaluated to account for humidity-induced changes in inter-fiber interactions and flow behavior. Furthermore, because cellulose powders are commonly used in combination with hydrophobic polymer matrices (Hubbe *et al.* 2008), the influence of hydrophobization was investigated. Through this approach, the flowability of various cellulose powders can be assessed by simultaneously considering multiple factors and evaluating both static and dynamic flow behaviors for applications such as reinforcing materials in composites, pharmaceutical excipients, and other related fields.

EXPERIMENTAL

Materials

A 2 wt% 2,2,6,6-tetramethylpiperidine-1-oxyl radical (TEMPO)-oxidized cellulose nanofiber suspension, manufactured by Moorim P&P (Ulsan, Korea), was dried in the laboratory using a spray dryer (SD-basic spray dryer, Lab plant, Huddersfield, UK), and the resulting powder was designated as "S_TOCN". The spray drying condition was as follows: an inlet temperature of 190 °C, an outlet temperature of 100 °C, and a suspension feed rate of 10 mL/min using a silicone nozzle with a diameter of 5 mm. In addition, TEMPO-oxidized cellulose nanofiber powder (TOCN) that had been dried at the Moorim P&P mill (Ulsan, Korea) was used for comparison. Microcrystalline cellulose, Avicel PH 101 (MCC), was purchased from Sigma-Aldrich (USA). Milled kenaf fiber (Kenaf) prepared by mechanical milling of original kenaf fibers without cooking or bleaching was

also used. Alkyl ketene dimer (AKD) emulsion (Kemira, Helsinki, Finland) with a solids content of 20% was used for hydrophobization of cellulose.

Classification of Powders by Particle Size

To analyze the effects of morphological characteristics on the flowability of powders, samples with various sizes and shapes were classified using 100-, 140-, and 500-mesh sieves. Through this classification, the powders were separated into several size grades. The volume mean diameter ($D[4.3]$) of the classified powders was measured using a particle size analyzer (Mastersizer 2000, Malvern Panalytical Ltd., Malvern, UK). In addition, scanning electron microscope (SEM, SUPRA 55VP, Carl Zeiss AG, Oberkochen, Germany) images were obtained at an accelerating voltage of 2 kV, and the aspect ratio was determined by image analysis using ImageJ software. The aspect ratio was calculated based on measurements of at least 100 particles for each sample.

Mixing Powders

To evaluate the influence of particle size distribution on flow properties, S_TOCN and MCC (Avicel PH) were mixed according to various mixing ratios (S_TOCN:MCC = 0:100 to 100:0). The powders were homogeneously mixed prior to analysis. The particle size and size distribution were analyzed using a particle size analyzer. The width of the size distribution (span) was used as a representative parameter for the size distribution, as defined in Eq. 1,

$$\text{Span} = \frac{[D(v,0.9) - D(v,0.1)]}{D(v,0.5)} \quad (1)$$

where $D(v, 0.1)$, $D(v,0.5)$, and $D(v,0.9)$ represent the particle diameters at which 10%, 50%, and 90% of the cumulative particle volume are reached, respectively.

Control of Moisture Content

The effect of moisture content on the flowability of powders was investigated using S_TOCN, TOCN, and MCC (Avicel PH). The moisture content of the powders was adjusted by placing them in a humidity-controlled chamber with various relative humidity (RH) levels (10 to 75%RH) at 23 °C for 8 h until the equilibrium moisture content (EMC) was reached.

Hydrophobization of Cellulose Powder

MCC (Avicel pH) was hydrophobized with AKD emulsion. A total of 500 g of AKD emulsion solutions with different concentrations ranging from 0.001 to 0.5 wt% (based on emulsion solids) were prepared using deionized water. Next, 20 g of MCC was added to each AKD emulsion solution and stirred at 200 rpm for 10 min with a magnetic stirrer. The treatment was carried out under neutral pH (approximately pH 7) and room temperature conditions. After the reaction, the powder was filtered by vacuum filtration and cured at 105 °C for 2 h.

Measurement of the Amount of Adsorbed AKD

The amount of adsorbed AKD was determined from the turbidity of the solution before and after the reaction. The turbidity was measured using a turbidimeter (2100AN, Hach, Loveland, USA). Turbidity at various concentrations of the AKD emulsion was measured to construct a calibration curve. Based on the calibration curve, the amount of

AKD adsorbed onto MCC was calculated according to the concentration of AKD emulsion. The equation of the calibration curve can be seen in Eq. 2,

$$\text{Turbidity (NTU)} = 43188 x + 0.18 \quad (R^2=0.9946) \quad (2)$$

where x is the concentration of AKD emulsion (%).

Removal of Unbound AKD

Hydrolyzed unbound AKD can reduce the friction coefficient (Karamdemir *et al.* 2004). Therefore, the presence of residual AKD may affect the flowability. To investigate the effect of unbound AKD, the hydrophobized cellulose powder (MCC) was immersed in toluene at a solvent-to-powder mass ratio of 100:1 for 3 h, followed by vacuum filtration. The resulting cellulose was then air-dried at 23 °C.

Measurement of Flowability

Angle of repose

To evaluate the static flowability of the powder, the angle between the pile of powder formed after being discharged through a funnel and the horizontal plane was measured. The angle of repose is also an indicator of the cohesiveness of granular materials (Cain 2000). The funnel diameter was 10 mm, and the distance between the funnel nozzle and the horizontal plane was set to 55 mm.

Avalanche behavior (rotating drum measurement)

The dynamic flowability of the powder was investigated using a revolution powder analyzer (Revolution, Mercury Scientific Inc, Newtown, USA). This method measures the avalanche behavior of powders in a rotating drum. Through this analysis, the flowability of the powders was quantitatively assessed. For each measurement, a fixed volume of powder (25 mL) was weighed and then loaded into the drum, and the rotation speed of the drum was set to 0.3 rpm. The variation in the potential energy of the powder during rotation was recorded. All flowability measurements were conducted at 23 °C. In this study, the avalanche energy, avalanche energy standard deviation, and cohesion-T were used as indicators of flowability. Avalanche energy refers to the amount of energy released by an avalanche of powder and is directly related to flowability. Avalanche energy standard deviation (avalanche energy std) is a parameter that indicates how consistently the powder flows. Cohesion-T is related to the cohesiveness of the powder, as described in detail by Gao *et al.* (2021).

RESULTS AND DISCUSSION

Effect of Morphological Properties

To evaluate the flowability of the powders depending on the morphological properties, the particle size and aspect ratio of the classified powder were measured. As shown in Fig. 1, the powders exhibited various shapes and sizes depending on the types of cellulose, and Table 1 summarizes their corresponding size and aspect ratio. The powder produced by spray drying the nanocellulose suspension (S_TOCN) had a spherical shape and passed through all sieves. The size and aspect ratio of S_TOCN were 11.6 μm and 1.34, respectively, making it the smallest among the samples. TOCN had a similar morphology to S_TOCN but a larger particle size (41.1 μm). TOCN powders were classified using 500-

mesh and 140-mesh sieves, and their aspect ratios ranged from 1.3 to 1.4. MCC exhibited an average particle size of 81.6 μm and an aspect ratio between 2 and 3, with a standard deviation greater than that of TOCN. The particles had an irregular shape. Kenaf powder showed the largest size and aspect ratio, retaining its original fibrous, rod-like morphology. Even when passed through the same sieve, the particle size of Kenaf remained larger than that of other powders. Compared with microcrystalline cellulose (Nechyporchuk *et al.* 2016), flexible cellulose nanofibers (S_TOCN and TOCN) were transformed into more spherical powders by spray drying.

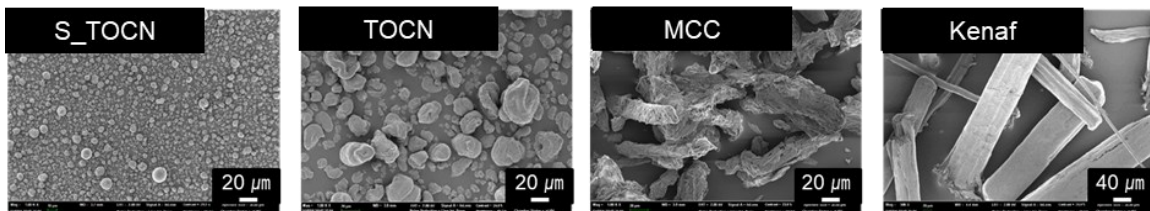


Fig. 1. SEM images of cellulose powders

Table 1. Properties of Classified Powders

Powder	Properties	Before classification	< 500 mesh	140 to 500 mesh	100 to 140 mesh
S_TOCN	D[4.3] (μm)	11.6	11.6	-	-
	Aspect ratio	1.34 \pm 0.21	1.34 \pm 0.21	-	-
TOCN	D[4.3] (μm)	41.1	29.5	45.8	-
	Aspect ratio	1.36 \pm 0.27	1.31 \pm 0.19	1.39 \pm 0.22	-
MCC	D[4.3] (μm)	81.6	27.5	73.3	87.8
	Aspect ratio	2.31 \pm 0.83	2.01 \pm 0.83	2.40 \pm 1.14	2.41 \pm 1.24
Kenaf	D[4.3] (μm)	187.8	65.2	173.5	189.9
	Aspect ratio	5.77 \pm 2.21	3.66 \pm 2.13	5.97 \pm 2.77	5.40 \pm 1.81

The flowability of the classified cellulose powders was evaluated using both the angle of repose and a revolution powder analyzer. Figure 2 shows the flowability results of the classified powders, illustrating how particle size and aspect ratio influence flow behavior. The angle of repose of the cellulose powder ranged from 40° to 60° (Fig. 2a), indicating flowability levels from passable to very poor (Riley and Hausner 1970). As the particle size increased up to approximately 70 μm , the angle of repose decreased from 60° to 43°. It is clear that the angle of repose of TOCN, MCC, and Kenaf decreased with increasing particle size, suggesting that larger particles exhibit better flowability. When particle sizes were comparable (approximately within 70 μm), the angle of repose followed the order kenaf > MCC > TOCN, indicating that powders with higher aspect ratios exhibited relatively poorer flowability (higher angle of repose). However, when the particle size exceeded 70 μm , the angle of repose remained nearly constant. This means that the influence of aspect ratio became negligible, and flowability approached a constant value.

Results obtained from the revolution powder analyzer (Figs. 2b, c, and d) supported these observations. During the test, severe sticking was observed in S_TOCN (Fig. 2e). Except for S_TOCN, the trends in avalanche energy, avalanche energy std, and cohesion-T were consistent with the angle of repose results. Figures 2b, c, and d show that as the particle size increased up to 70 μm , all three parameters decreased remarkably and then leveled off. These findings indicate that increasing particle size improved flowability and

resulted in more powder uniform. The aspect ratio, however, had little effect on the dynamic rotational behavior.

Overall, both static and dynamic flowability improved with increasing particle size. This improvement was attributed to the reduced contact area and van der Waals interactions between larger particles, combined with the greater gravitational force acting on the powder. Spherical particles with lower aspect ratios also exhibited enhanced flowability due to reduced interparticle friction. Nevertheless, the effects of particle shape and aspect ratio on flowability were less pronounced compared to particle size. Regardless of other morphological characteristics, cellulose powders with particle sizes above 70 μm exhibited consistent flow behavior.

Recently, nanofibrillated cellulose has been explored as a reinforcing fiber for lightweight and high strength biocomposites. However, based on the results shown in Fig. 2, uniform and rapid feeding of nanocellulose may be challenging due to its small particle size. Therefore, strategies to improve the flowability of nanocellulose powder, such as incorporating inorganic additives, should be considered.

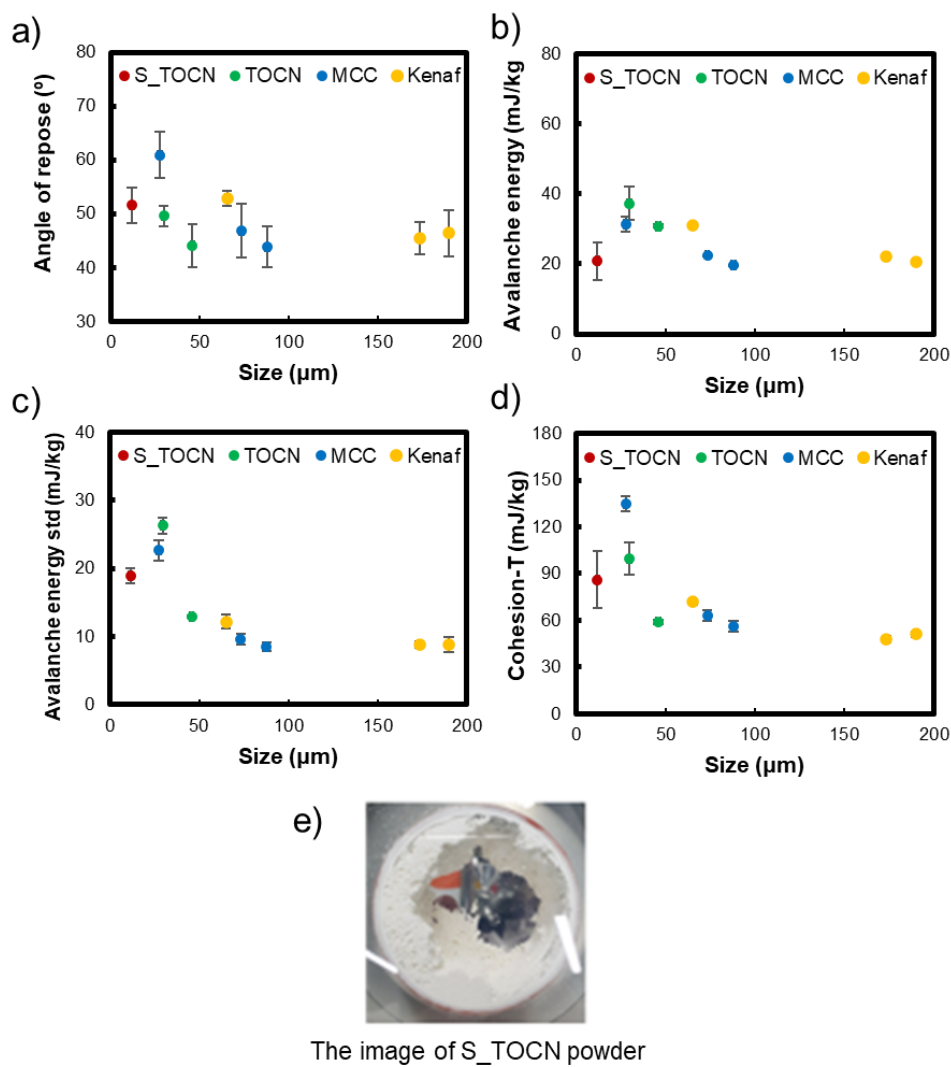


Fig. 2. Flowability of classified cellulose powders: a) Angle of repose, b) Avalanche energy, c) Avalanche energy standard deviation, d) Cohesion-T, e) S_TOCN observed in a rotating drum

Effect of Size Distribution

Figure 3 presents the particle size distribution, span, and average particle size of mixed cellulose powders (S_TOCN/MCC) depending on the S_TOCN content. Both S_TOCN and MCC exhibited unimodal particle size distribution. In contrast, mixtures containing 20 to 50% S_TOCN showed bimodal distributions with high span values (> 4). The average particle size of the mixture decreased from 81.6 μm to 11.6 μm as the proportion of S_TOCN increased.

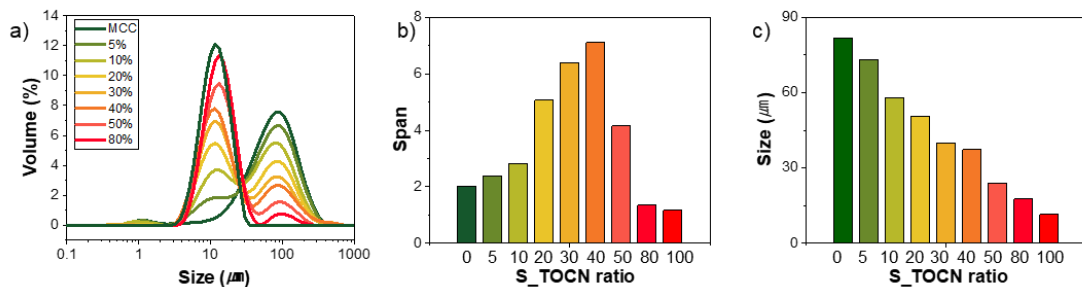


Fig. 3. Particle size distribution and average particle size of mixed cellulose powders depending on the S_TOCN content: a) Particle size distribution; b) Span of particle size distribution; c) Average particle size

The flowability of the mixed powders, evaluated using both static and dynamic methods, is presented in Fig. 4. Figure 4a shows the angle of repose as a function of span. For powders with unimodal particle size distribution, the angle of repose primarily depended on the dominant component (*i.e.*, S_TOCN ratios of 0 to 10% or 80 to 100%). When the size distribution was broad or bimodal, the powders exhibited higher angles of repose (50 to 60°), indicating very poor flowability.

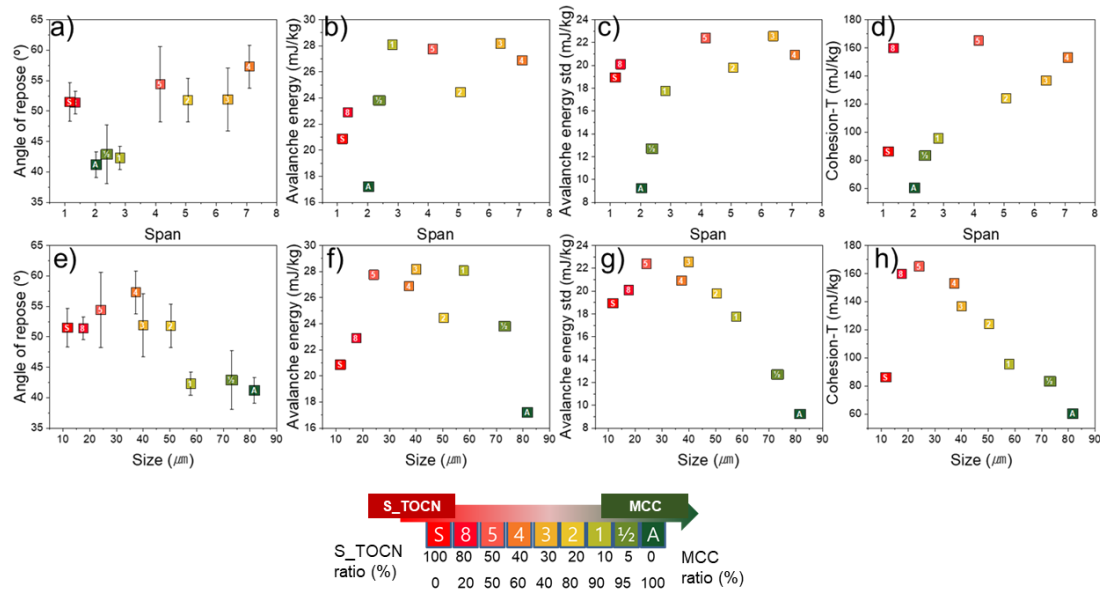


Fig. 4. Flowability of mixed cellulose powders depending on (a through c) span and (d through f) average particle size; (a, d) Angle of repose, (b, e) Avalanche energy, (c, f) Cohesion-T

However, it was difficult to find a clear relationship between span and angle of repose. In contrast, the avalanche behavior of the powders (Figs. 4b and 4c) showed a noticeable relationship with span. Except for very fine powders (S_TOCN content > 50%), the flowability decreased with increasing span value. Figures 4 d, e, and f present the flowability results depending on the particle size.

As shown in Fig. 4d, the angle of repose decreased with increasing particle size, indicating improved flowability. Moreover, particle size exhibited a stronger correlation with the angle of repose than did span. The avalanche behavior of the mixed powders as a function of their average particle size (Figs. 4e and 4f) further supported this trend, showing that dynamic flowability improved with increasing particle size. Consequently, the results in Fig. 4 indicate that although powders with broader size distribution generally showed poorer flowability, the degree of size distribution was not directly proportional to flowability. Particle size had a greater effect on both static and dynamic flow properties than size distribution.

Effect of Moisture Content

The equilibrium moisture content (EMC) of the cellulose powders is shown in Fig. 6a. Although S_TOCN and TOCN had the same chemical composition, the EMC of S_TOCN was higher due to its smaller particle size and higher specific surface area. In contrast, the relatively larger MCC powder exhibited a lower EMC value than S_TOCN and TOCN, which can be attributed to its lower specific surface area and different surface chemical composition.

Figure 6b presents the flowability of S_TOCN as a function of moisture content. At higher moisture contents, the avalanche energy, avalanche energy standard deviation, and cohesion-T decreased, indicating improved flowability. At low moisture content, sticking occurred due to the accumulation of static charges. As the moisture content increased, this tendency diminished; however, agglomeration between powder particles was observed.

Because agglomerated powders behave like larger particles, the powders with higher moisture content exhibited better flowability. This suggests that water not only reduces the electrostatic interaction but also promotes interparticle agglomeration. Figures 6c and 6d shows the avalanche behavior of TOCN and MCC powders depending on the moisture content. For these powders, avalanche energy, avalanche energy standard deviation, and cohesion-T all increased with increasing moisture content. Unlike S_TOCN, TOCN powders with relatively larger particle sizes and smaller surface areas experienced less electrostatic force at lower moisture content. As the moisture content increased, however, liquid bridges formed between particles, enhancing cohesion and thus worsening flowability.

In summary, the effect of moisture content on the flowability of cellulose powder varied depending on particle size. For small particles (< 20 μm), increasing moisture content reduced electrostatic force and promoted agglomeration, causing the powders to flow more like larger particles (Fig. 6e). Conversely, for larger powders, such as TOCN and MCC, higher moisture content increased interparticle cohesion through water-mediated liquid bridges, leading to reduced flowability.

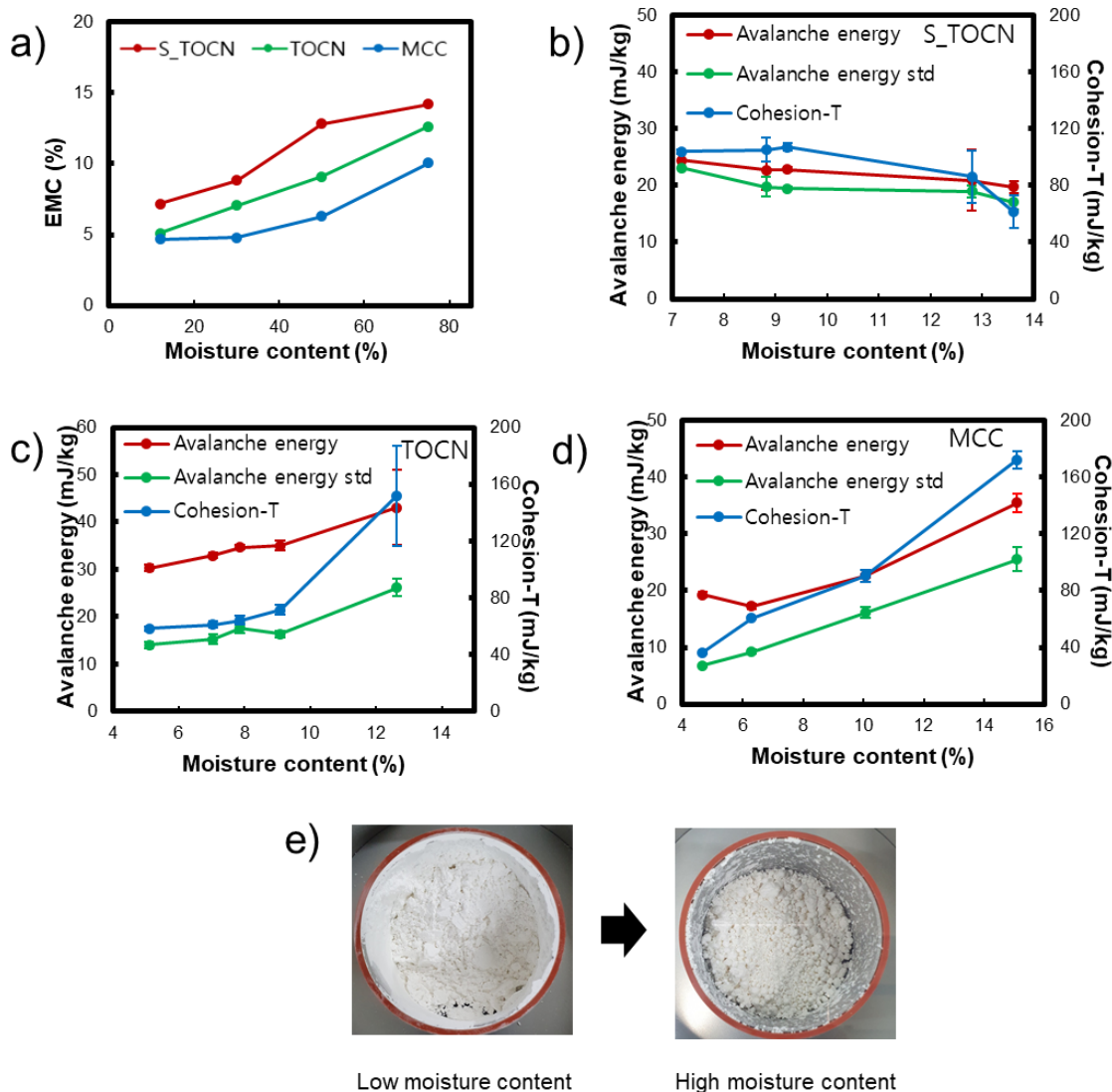


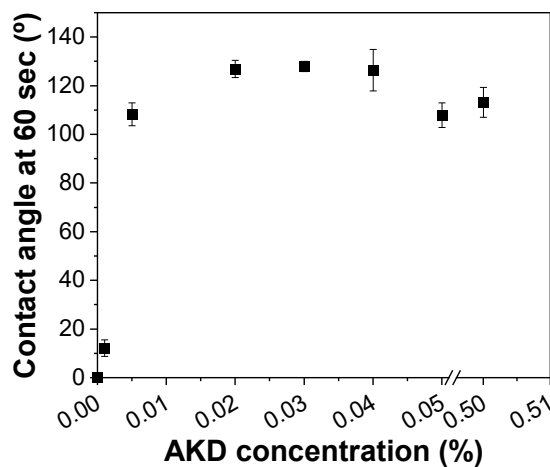
Fig. 6. Flowability of cellulose powders as a function of moisture content: a) Equilibrium moisture content of cellulose powders; b) Flowability of S_TOCN; c) Flowability of TOCN; d) Flowability of MCC; e) Appearance of S_TOCN powders at different moisture contents

Effect of AKD Hydrophobization

To investigate the effect of powder surface chemistry on flowability, MCC was hydrophobized with an AKD emulsion. Table 2 presents the amount of adsorbed AKD, calculated from the calibration curve derived from turbidity measurements. As the concentration of AKD emulsion increased, the amount of AKD adsorbed onto MCC also increased, eventually reaching a plateau. Adsorption reached near saturation at an AKD emulsion concentration of approximately 0.04%, after which further adsorption proceeded slowly. Meanwhile, the contact angle as a function of adsorbed AKD per unit mass of MCC (Fig. 7) remained nearly constant (100 to 130°) when the adsorbed AKD per MCC exceeded 1.2 mg/g (corresponding to an AKD reaction concentration of 0.005%). This indicates that once the adsorbed AKD per MCC surpassed 1.2 mg/g, the surface energy of the hydrophobized cellulose powder remained similar regardless of further AKD adsorption.

Table 2. Amount of Adsorbed AKD onto MCC

AKD Concentration (%)	Residual AKD (mg)	Adsorbed AKD (mg)	Adsorbed AKD per MCC (mg/g)
0.001	0.2	4.9	0.2
0.005	0.2	24.9	1.2
0.02	3.2	96.8	4.8
0.03	46.0	104.0	5.2
0.04	90.6	109.4	5.5
0.05	135.8	114.2	5.7
0.5	2360.5	139.5	7.0

**Fig. 7.** Contact angle of hydrophobized MCC cellulose powder as a function of AKD concentration

The flowability of hydrophobized MCC was evaluated using the angle of repose and a revolution powder analyzer. As shown in Figs. 8a, b, and c, the angle of repose, avalanche energy, and avalanche energy standard deviation decreased with increasing AKD concentration up to 0.04%. This result is consistent with previous findings that AKD reduces friction in paper manufacturing processes (Karademir *et al.* 2004). However, when the cellulose powder was treated with AKD emulsion concentrations above the saturation point, excessive AKD adsorption led to a deterioration in flowability. This behavior can be explained by changes in surface energy: while hydrophobization reduces the surface energy of cellulose powder and thereby enhances flowability, excessive AKD adsorption can disrupt the smooth flow of particles.

It appears that strong interactions between cellulose particles arise from the affinity or friction between AKD layers. Although the contact angle remained nearly constant regardless of the amount of adsorbed AKD per unit mass of MCC (Fig. 7), the flowability varied with the degree of AKD adsorption. In summary, while reducing surface energy through hydrophobization can improve the flowability, excessive AKD treatment can have the opposite effect, hindering the flow of cellulose powder.

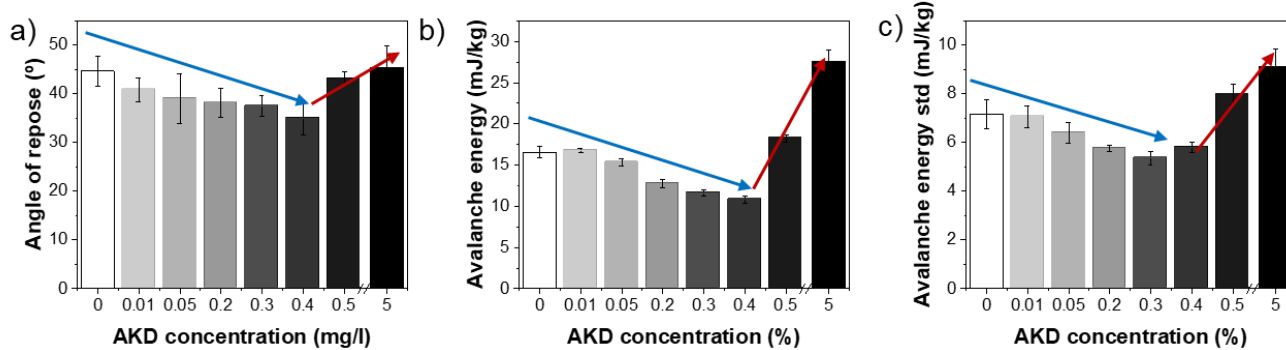


Fig. 8. Flowability of hydrophobized MCC depending on AKD concentration: a) Angle of repose; b) Avalanche energy; c) Avalanche energy std

To examine the effect of unbound AKD on the flowability of cellulose powder, hydrophobized cellulose powder was washed with toluene to remove unbound AKD, and the flowability before and after washing was compared. Figure 9a shows the avalanche energy, and Fig. 9b shows the avalanche energy standard deviation. Both parameters decreased after toluene washing. When the reaction AKD concentration exceeded 0.04%, the reduction in avalanche energy and its standard deviation was pronounced. When the amount of adsorbed AKD was low (AKD concentration < 0.04%), the difference in flowability before and after washing was not great. However, at higher adsorption levels (AKD concentration > 0.05%), the flowability improved substantially after washing. These results indicate that removing unbound AKD enhances the flowability of cellulose powder. This observation is consistent with the findings of Karademir *et al.* (2004), which reported that the unbound AKD exhibits a higher friction coefficient than bound AKD. Therefore, removing unbound AKD while retaining bound AKD on the cellulose surface efficiently improved the flowability of cellulose powder.

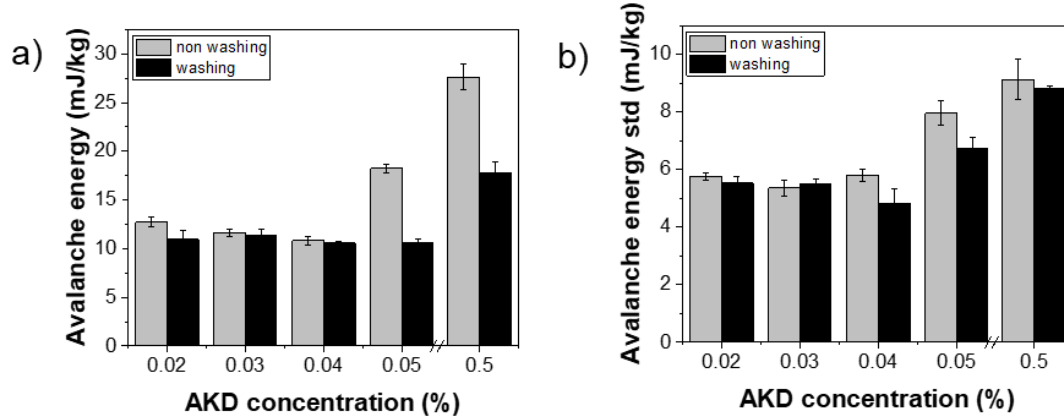


Fig. 9. Comparison of the flowability of hydrophobized cellulose powder before and after toluene washing: a) Avalanche energy; b) Avalanche energy std

CONCLUSIONS

1. The effects of morphological properties (particle size, size distribution, and shape), moisture content, and hydrophobization treatment on the flowability of TEMPO-oxidized cellulose nanofibers (S_TOCN and TOCN), microcrystalline cellulose (MCC), and milled kenaf (Kenaf) powders were evaluated using the angle of repose and a revolution powder analyzer.
2. Among the various morphological factors, the particle size was identified as the most important factor influencing the flowability of cellulose powders. As particle size increased, the angle of repose decreased from approximately 60° to 45°, while the avalanche energy decreased from 37 to 20 mJ/kg. When the size exceeded approximately 70 µm, flowability remained nearly constant. Spherical powder exhibited better flowability than rod-shaped powder. Although a more uniform particle size distribution tended to enhance flowability, the effect of size distribution was less pronounced compared to that of particle size.
3. To examine the influence of the moisture content, cellulose powders were conditioned under various relative humidity levels. The effect of humidity on moisture uptake varied depending on the particle size of the cellulose powders. As the moisture content of cellulose powder increased, S_TOCN powders with particle sizes below 20 µm exhibited improved flowability, whereas the flowability of relatively larger powders deteriorated.
4. Finally, the effect of hydrophobization with AKD was evaluated. Hydrophobization, which reduced the surface energy of the powder, improved the flowability of MCC. However, excessive AKD adsorption ($> 5.5 \text{ mg/g}_{\text{cellulose}}$) hindered smooth flow of powders. The removal of unbound AKD through toluene washing further enhanced the flowability of cellulose powders.

ACKNOWLEDGMENTS

This work was by the 'Industrial Technology Innovation Program (No. 20010431)' funded by the Ministry of Trade, Industry and Energy (MOTIE, Korea) and 'R&D Program for Forest Science Technology (KOFPI2020214C10-2022-AC01)' provided by Korea Forest Service (Korea Forestry Promotion Institute, Korea).

Conflict of Interest

The authors declare that they have no known competing financial interests or personal relationships that could have appeared to influence the work reported in this paper.

REFERENCES CITED

Amidon, G. E., and Houghton, M. E. (1995). "The effect of moisture on the mechanical and powder flow properties of microcrystalline cellulose," *Pharmaceutical Research* 12(6), 923-929. <https://doi.org/10.1023/A:1016233725612>

Brubaker, J., and Moghtadernejad, S. (2024). "A comprehensive review of the rheological properties of powders in pharmaceuticals," *Powders* 3(2), 233-254.

Cain, J. (2000). "An alternative technique for determining ANSI," *CEMA Standard* 550, 218-220.

Chattoraj, S., Shi, L., and Sun, C. C. (2011). "Profoundly improving flow properties of a cohesive cellulose powder by surface coating with nano-silica through comilling," *Journal of Pharmaceutical Sciences* 100(11), 4943-4952.

Crouter, A., and Briens, L. (2014). "The effect of moisture on the flowability of pharmaceutical excipients," *AAPS PharmSciTech* 15(1), 65-74. <https://doi.org/10.1208/s12249-013-0036-0>

Faqih, A. M. N., Mehrotra, A., Hammond, S. V., and Muzzio, F. J. (2007). "Effect of moisture and magnesium stearate concentration on flow properties of cohesive granular materials," *International Journal of Pharmaceutics* 336(2), 338-345. <https://doi.org/10.1016/j.ijpharm.2006.12.024>

Gao, M., Ludwig, B., and Palmer, T. (2021). "Impact of atomization gas on characteristics of austenitic stainless steel powder feedstocks for additive manufacturing," *Powder Technology* 383, 30-42. <https://doi.org/10.1016/j.powtec.2020.12.005>

Geldart, D., Abdullah, E., Hassanpour, A., Nwoke, L., and Wouters, I. (2006). "Characterization of powder flowability using measurement of angle of repose," *China Particuology* 4(3-4), 104-107. [https://doi.org/10.1016/S1672-2515\(07\)60247-4](https://doi.org/10.1016/S1672-2515(07)60247-4)

Genina, N., Räikkönen, H., Heinämäki, J., Antikainen, O., Siiriä, S., Veski, P., and Yliruusi, J. (2009). "Effective modification of particle surface properties using ultrasonic water mist," *AAPS PharmSciTech* 10(1), 282-288.

Genina, N., Räikkönen, H., Ehlers, H., Heinämäki, J., Veski, P., and Yliruusi, J. (2010). "Thin-coating as an alternative approach to improve flow properties of ibuprofen powder," *International Journal of Pharmaceutics* 387(1-2), 65-70.

Hancock, B. C., Vukovinsky, K. E., Brolley, B., Grimsey, I., Hedden, D., Olsofsky, A., and Doherty, R. A. (2004). "Development of a robust procedure for assessing powder flow using a commercial avalanche testing instrument," *Journal of Pharmaceutical and Biomedical Analysis* 35(5), 979-990. <https://doi.org/10.1016/j.jpba.2004.02.035>

Hassan, M. S., and Lau, R. W. M. (2009). "Effect of particle shape on dry particle inhalation: Study of flowability, aerosolization, and deposition properties," *AAPS PharmSciTech* 10(4), 1252-1262. <https://doi.org/10.1208/s12249-009-9313-3>

Horio, T., Yasuda, M., and Matsusaka, S. (2014). "Effect of particle shape on powder flowability of microcrystalline cellulose as determined using the vibration shear tube method," *International Journal of Pharmaceutics* 473(1-2), 572-578. <https://doi.org/10.1016/j.ijpharm.2014.07.040>

Hubbe, M. A., Rojas, O. J., Lucia, L. A., and Sain, M. (2008). "Cellulosic nanocomposites: A review," *BioResources* 3(3), 929-980.

Jenike, A. W. (1964). *Storage and Flow of Solids*, Bulletin No 123, Utah State University.

Karademir, A., Hoyland, D., Wiseman, N., and Xiao, H. (2004). "A study of the effects of alkyl ketene dimer and ketone on paper sizing and friction properties," *APPITA Journal* 57(2), 116-120.

Kim, J.-H., Kim, U.-S., Han, K.-S., and Hwang, K.-T. (2019). "Effect of hydrophobic surface coating on flowability of ceramic tile granule powders," *Korean Journal of Materials Research* 29(7), 425-431. <https://doi.org/10.3740/MRSK.2019.29.7.425>

Kudo, Y., Yasuda, M., and Matsusaka, S. (2020). "Effect of particle size distribution on flowability of granulated lactose," *Advanced Powder Technology* 31(1), 121-127. <https://doi.org/10.1016/j.apt.2019.10.004>

Lavoie, F., Cartilier, L., and Thibert, R. (2002). "New methods characterizing avalanche behavior to determine powder flow," *Pharmaceutical Research* 19(6), 887-893. <https://doi.org/10.1023/A:1016125420577>

Li, Q., Rudolph, V., Weigl, B., and Earl, A. (2004). "Interparticle van der Waals force in powder flowability and compactibility," *International Journal of Pharmaceutics* 280(1-2), 77-93. <https://doi.org/10.1016/j.ijpharm.2004.05.001>

Liu, L., Marziano, I., Bentham, A., Litster, J., White, E., and Howes, T. (2008). "Effect of particle properties on the flowability of ibuprofen powders," *International Journal of Pharmaceutics* 362(1-2), 109-117. <https://doi.org/10.1016/j.ijpharm.2008.06.023>

Mehta, A., and Barker, G. (1994). "The dynamics of sand," *Reports on Progress in Physics* 57(4), Article Number 383. <https://doi.org/10.1088/0034-4885/57/4/002>

Monroe, J. E., Kumar, D. S., and Emady, H. N. (2025). "Evaluation of flow properties of wetted microcrystalline cellulose using the FT4 Powder Rheometer: Insights into limiting behaviors," *Powder Technology* 464, 121161.

Nechyporchuk, O., Belgacem, M. N., and Bras, J. (2016). "Production of cellulose nanofibrils: A review of recent advances," *Industrial Crops and Products* 93, 2-25. <https://doi.org/10.1016/j.indcrop.2016.02.016>

Nevell, T. P., and Zeronian, S. H. (1985). *Cellulose Chemistry and Its Applications*, Ellis Horwood Ltd., Chichester, UK.

Ohwoavworhua, F. O., and Augustine, O. O. (2020). "Cellulose nanocrystals and nanofibrils obtained from corn straw by hydrolytic action of four acids: particulate, powder and tablet properties," *Drug Discovery* 14(34), 314-327.

Orts, W. J., Shey, J., Imam, S. H., Glenn, G. M., Guttman, M. E., and Revol, J.-F. (2005). "Application of cellulose microfibrils in polymer nanocomposites," *Journal of Polymers and the Environment* 13(4), 301-306. <https://doi.org/10.1007/s10924-005-5514-3>

Peleg, M. (1977). "Flowability of food powders and methods for its evaluation—a review," *Journal of Food Process Engineering* 1(4), 303-328. <https://doi.org/10.1111/j.1745-4530.1977.tb00188.x>

Peng, Y., Gardner, D. J., and Han, Y. (2012). "Drying cellulose nanofibrils: In search of a suitable method," *Cellulose* 19(1), 91-102. <https://doi.org/10.1007/s10570-011-9630-z>

Prescott, J. K., and Barnum, R. A. (2000). "On powder flowability," *Pharmaceutical Technology* 24(10), 60-85.

Riley, R., and Hausner, H. (1970). "Effect of particle size distribution on the friction in a powder mass," *International Journal of Powder Metallurgy* 6, 17-22.

Shah, D. S., Moravkar, K. K., Jha, D. K., Lonkar, V., Amin, P. D., and Chalikwar, S. S. (2023). "A concise summary of powder processing methodologies for flow enhancement," *Heliyon* 9(6), e16498.

Sharifi, F., Mahmoodi, Z., Abbasi, S. M., Najafi, A., and Khalaj, G. (2023). "Synthesis and characterization of mesoporous TiC nanopowder/nanowhisker with low residual carbon processed by sol-gel method," *Journal of Materials Research and Technology* 22, 2462-2472.

Shokri, J., and Adibkia, K. (2013). "Application of cellulose and cellulose derivatives in pharmaceutical industries," in: *Cellulose – Medical, Pharmaceutical and Electronic Applications*, IntechOpen, London, UK.

Stavrou, A. G., Hare, C., Hassanpour, A., and Wu, C.-Y. (2020). "Investigation of powder flowability at low stresses: Influence of particle size and size distribution," *Powder Technology* 364, 98-114. <https://doi.org/10.1016/j.powtec.2020.01.068>

Sun, C. C. (2016). "Quantifying effects of moisture content on flow properties of microcrystalline cellulose using a ring shear tester," *Powder Technology* 289, 104-108.

Tasnim, S., Tipu, M. F. K., Rana, M. S., Rahim, M. A., Haque, M., Amran, M. S., and Chowdhury, J. A. (2023). "Modification of bulk density, flow property and crystallinity of microcrystalline cellulose prepared from waste cotton," *Materials* 16(16), article 5664.

Trpělková, Ž., Hurychová, H., Kuentz, M., Vraníková, B., and Šklubalová, Z. (2020). "Introduction of the energy to break an avalanche as a promising parameter for powder flowability prediction," *Powder Technology* 375, 33-41. <https://doi.org/10.1016/j.powtec.2020.07.095>

Turbak, A. F., Snyder, F. W., and Sandberg, K. R. (1983). "Microfibrillated cellulose, a new cellulose product: Properties, uses, and commercial potential," *Journal of Applied Polymer Science: Applied Polymer Symposia* 1983, 815-827.

Zafeiropoulos, N. E. (2011). *Interface Engineering of Natural Fibre Composites for Maximum Performance*, Woodhead Publishing, Sawston, UK.

Zainuddin, I. M., Yasuda, M., Horio, T., and Matsusaka, S. (2012). "Experimental study on powder flowability using vibration shear tube method," *Particle & Particle Systems Characterization* 29(1), 8-15. <https://doi.org/10.1002/ppsc.201100052>

Zhang, X., Wu, X., Gao, D., and Xia, K. (2012). "Bulk cellulose plastic materials from processing cellulose powder using back pressure-equal channel angular pressing," *Carbohydrate Polymers* 87(4), 2470-2476. <https://doi.org/10.1016/j.carbpol.2011.11.019>

List of Abbreviations

TEMPO	2,2,6,6-tetramethylpiperidine-1-oxylradical
S_TOCN	TEMPO-oxidized cellulose nanofiber powder dried using a laboratory spray dryer
TOCN	TEMPO-oxidized cellulose nanofiber powder
MCC	Microcrystalline cellulose, Avicel PH 101
Kenaf	Milled kenaf fiber
AKD	Alkyl ketene dimer
D[4.3]	Volume mean diameter
SEM	Scanning electron microscope
Span	Width of the size distribution
D(v, 0.1)	Particle diameter at 10% cumulative volume
D(v, 0.5)	Particle diameter at 50% cumulative volume
D(v, 0.9)	Particle diameter at 90% cumulative volume
EMC	Equilibrium moisture content
Avalanche energy	Amount of energy released by an avalanche of powder
Avalanche energy std	Avalanche energy standard deviation
Cohesion-T	Cohesiveness of the powder

Article submitted: Nov. 10, 2025; Peer review completed: December 13, 2025; Revised version received: December 16, 2025; Accepted: December 19, 2025; Published: December 29, 2025.

DOI: 10.15376/biores.21.1.1397-1412